Baba, R., Jacobs, K. J.P., Stevens, B. J., Harisson, B. A., Watt, A. P., Mukai, T. and Hogg, R. A. (2019) Resonant Tunnelling Diodes for Next Generation THz Systems. In: 2018 IEEE British and Irish Conference on Optics and Photonics (BICOP), London, UK, 12-14 Dec 2018, ISBN 9781538673614.

Resonant Tunnelling Diodes for next-generation THz systems

Răzvan Baba
School of Engineering
University of Glasgow
Glasgow, UK
elp13rb@gmail.com

Kristof J.P. Jacobs
Department of Electronic &
Electrical Engineering
The University of Sheffield
Sheffield, UK
elp11kjj@gmail.com

Ben J. Stevens
IQE Photonics
IQE plc.
Cardiff, UK
stevens.ben@gmail.com

Brett A. Harrison
National Epitaxy Facility
The University of Sheffield
Sheffield, UK
b.a.harrison@sheffield.ac.uk

Adam P. Watt
School of Engineering
University of Glasgow
Glasgow, UK
a.watt.1@research.gla.ac.uk

Toshikazu Mukai
Manufacturing Division
ROHM Co., Ltd.
Kyoto, Japan
toshikazu.mukai@mnf.rohm.co.jp

Richard A. Hogg
School of Engineering
University of Glasgow
Glasgow, UK
richard.hogg@glasgow.ac.uk

***Abstract*— Resonant tunnelling diodes (RTDs) are a strong candidate for future wireless communications in the THz spectrum (sub-millimetre waves), offering compact, room-temperature operation with the potential to exceed the bit transfer rate mandated by the 12G-SDI standard, using a single wireless link. A free-space RTD emitter operating at 353GHz is described. The fabrication process consists of a dual-pass I-line photolithography & etch technique using an air bridge, allowing low resistivity ohmic contacts, and accurate control of desired device area. With extrinsic circuit elements taken into account, the intrinsic semiconductor efficiency is analysed to investigate structural improvements for radiative efficiency. Such optimised structures are presented, and then characterised after being epitaxially grown with commercially viable metal-organic vapour phase epitaxy (MOVPE) reactors. A combination of low temperature photoluminescence spectroscopy, X-Ray diffractometry, and transmission electron microscopy attest the quality of the new material. We end with a suggestion for the next steps to exceed technological readiness levels of 8, and use monolithic RTD emitters as components in new systems.**

Keywords—resonant tunnelling diode, terahertz emitters, core technologies, semiconductor fabrication, non-destructive characterisation

I. INTRODUCTION

The lower terahertz spectrum, spanning from approximately 0.1 to 3 THz (corresponding to wavelengths of 3 to 0.1 mm) is an under-exploited part of the electromagnetic spectrum, situated at the convergence of the light and microwave technologies. Because of this placement, it has traditionally been difficult to generate waves in this range through either photonic or electronic means, creating a gap in technology known as the 'terahertz gap'[1]. In the last 10 years alone, the outlook has changed significantly. However, despite constant wave sources either popularly based on Schottky multiplier chains, difference-frequency based on photonic mixing of 2 wavelength lasers, or even ultra-fast pulse laser systems being commercially available as table-top systems, currently there are no efficient, cost-effective, compact, high-power solid state sources which would fit inside a typical mobile phone.

Contemporary resonant tunnelling diodes (RTDs) are a case of a mesoscopic-scale semiconductor device with active regions <10 nm which are a strong contender to fill this requirement. Of the competing technologies, one can be reminded of unitravelling carrier photodiodes (UTC-PD)[2], [3], with powers of tens of μW, Gunn diodes [4], conventional Schottky diodes [5], high electron mobility transistors (HEMT) [6], as well as emerging plasmonics[7], and photonic crystals [8]. UTC-PDs do not typically offer a mechanism for phase coherence, and as such, THz radiation is collected by a hyper-hemispherical silicon lens in a typical application, limiting the scope of miniaturisation. The Gunn diode shares the same *n-i-n* doping scheme as the RTD, but without the added benefit of quantum confinement, and Schottky barrier detectors have been proven to be inferior to RTDs of modest structural quality[9]. HEMTs also lack mechanisms for phase coherence, but their development remains important for monolithic micro-integrated circuits. It is of note that most of these high frequency devices, whilst realisable in silicon, work most efficiently with direct band gap compound semiconductors. III-V semiconductors in particular, are a mature industry which is now reaching a half-centenary of existence thanks to the wide spread of media such as the CD/DVD, and today, the adoption of solid-state RGB LEDs. In our case, the InGaAs/AlAs on InP substrates system was chosen, as it provides the possibility of known, high-quality epitaxy, with high conduction-band offsets necessary for the quantum operation regimen of the RTD. The InP platform is also employed in 1.55μm laser emitters used for long-distance fibre communications.

The authors would like to acknowledge UKRC grants EP/503812/1 and EP/L505055/1 DTA studentship; the European Commission Horizon 2020 iBROW project 645369; University of Glasgow PGR Travel Scholarship Fund for the financial aid offered during this work.

Purely photonic-based techniques of generating THz tend to be significantly bulkier vs. electronic devices, with the requirements of meV energy level transitions imposing a regimen of low temperature operation. THz-quantum cascade lasers (THz-QCLs)[10], despite their high power and beam quality, are perhaps an example of this, where several of these advantages are lost typically >100 K through carrier back-population. They are more likely to find use in laboratory spectroscopy machines and upper atmosphere monitoring and space exploration. There are different constructions available for THz vacuum devices operating at arbitrary output power levels [1].

The challenge of exploiting the THz radiation is therefore far from over, and the problem is compounded by the strong absorption lines of the gases which compose the Terran atmosphere [11]. For short-distance communications in the foreseeable future, there are several potential windows available 75-110 (some bands already reserved), 125-180, 200-310, 330-415, 435-460 GHz, with severely increasing attenuation with increase in frequency. THz would offer advantages of powers in excess of 1mW at ~300GHz [12], high data rates, high directivity, particulate-matter resistance, and an added advantage of point-to-point security due to this atmospheric attenuation. Other areas of THz applications are included, but not limited to: combustion gas monitors [13], art conservation [14], health care [15], gas spectroscopy [16], industrial non-destructive testing [17], chemical identification & physical security [18]. Therefore, the RTD is one key part of this core of technologies with the potential to unlock a better quality of life for many.

II. THZ EMITTER AND ITS FABRICATION

A schematic of a RTD device used as an emitter is shown in Fig. 1. The RTD heterostructure itself is a pillar with diameters between 3 - 20 μm^2. In this case, no back-contact exists, and instead, an optimum dual-pass structure exists which allows very low resistivity, highly reproducible contacts to be formed. The top contact is connected via the means of a metal air bridge, and the other contact passes through another wafer path, practically acting as a passive bulk resistor [19]. The RTD element sits inside a slot antenna, and the wave is moderated by a metal-insulator-metal capacitor topology. Partial current oscillation stabilisation is achieved with a parallel resistor.

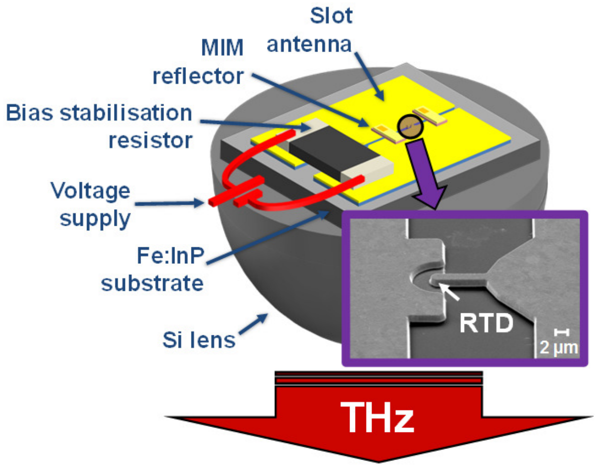

Fig. 1. (main) Schematic image of 0.35 THz emitter, demonstrated on a hyperhemispherical silicon lens for light collection, featured with an added quasi-stabilisation resistor. (inset) Shows an SEM micrograph mangifying the active RTD device, the semiconductor mesa of which is hidden under a metal air-bridge [19]

This layout has been used to demonstrate free-space emission, with a peak detected at 353 GHz [20], [21]. Unfortunately, at the time of the demonstration, ~97% of the THz radiation would be absorbed through the substrate, chiefly through free carrier absorption. To make matters worse, effective coupling of the radiation via a quarter wavelength transformer is not a trivial design job, and effectively limited by the overall negative differential resistance value of the RTD device itself.

III. EPITAXIAL OPTIMISATION

In order to better qualify & quantify the changes in device performance with modification to the epitaxial structure, a computer model of the RTD was set up. Working backwards from measurements, it was first necessary to determine the values of the extrinsic circuit elements, such as the contact resistance, the resistance due to the mesa topology, and compensate for other parasitics present in the system, such that the raw semiconductor I-V characteristic is obtained.

Fig. 2 presents an overview of the complex impedances associated with such a system [22]. The impedances correspond to that of the source (Z_s) copper traces and pads (Z_{tr}) leading to the component, the emitter and collector contacts (Z_{ce}, Z_{cc}), mesa and dual-pass layout (Z_{sheet}), the coupler (Z_c) and the antenna itself (Z_L) using successive wet etches, in the limit of a point-sized device (zero area), a peak voltage of 0.22V is determined, as well as the area-dependence onto the positive differential resistance region. With these 2 extra values, a more realistic fit to the I-V characteristics is possible than with the peak current density value alone. The zero-area limit appears due to the assumption of the simulator that the device is nominally identical in lateral directions, hence solving a 1-D problem.

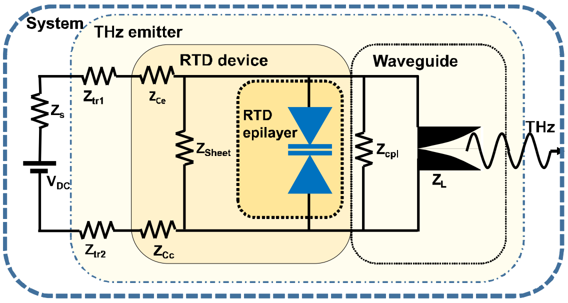

Fig. 2. A system diagram showing equivalent circuit model using complex impedances. The RTD THz emitter neglects the power source, and is compartmented in the semiconductor resonator device, and its radiating elements. The computer model solves the I-V characteristic (and other electron transport parameters) of the RTD epitaxial layers [22].

Taking into account the barrier width, quantum well (QW) width and well depth (*i.e.* the value of mole fraction x in the QW material $In_xGa_{1-x}As$), as well as imposing epitaxial strain limitations, we suggest an optimum device structure [22], with a thicker, shallower $In_{0.75}Ga_{0.25}As$ (~5nm – 17 atomic sheets), and very thin AlAs (~0.6 nm – 2 atomic sheets) barriers. A popular design alternative was also studied, where the QW is replaced with lattice-matched InGaAs and a region of pure InAs, finding similar improvements.

IV. NON-DESTRUCTIVE MATERIAL CHARACTERISATION

In order to evaluate the quality and potential yield (thus, profitability), the semiconductor industry employs highly customised, process-specific, automated wafer test tools. Fig. 3 presents low temperature photoluminescence spectra (15 K LT-PL) arranged in maps corresponding to a spectral output on a physical point on a 2 inch wafer. This tool is developed in-house, being capable of scanning 3 inch wafers at low temperature, or up to 4 inch wafers at room temperature. The shift in peak wavelength of 1467.69 ±4.38 nm is within a 1% precision tolerance of x of the bulk $In_xGa_{1-x}As$, whereas the small standard deviation of the signal intensity at the peak 1.1 ±0.11 (a.u.) is also a good indicator of overall epitaxial quality. Using the Moss-Burstein shift as an indicator, in previous work [23] we have also used LT-PL to verify the uniformity of doping. In this particular case estimated at 1.1×10^{19} carrier × cm^{-3} ±25%, after gross error was removed, also within design specification.

Characterising the bulk InGaAs is of limited usefulness with regards to the device performance. It is more important to determine the atomically thin layer structure that consists of the AlAs/InGaAs/AlAs double barrier-resonant tunnelling system (DBRTS). Previously, we presented [24] a way to partly overcome this challenge by introducing an electrically neutral copy of the active region buried beneath the bottom n++ contact. This would create a Type-II photonic transition in addition to the Type-I created by the initial DBRTS. The difference between the two would give the value of the elastic energy level E_1, the key parameter in regulating the RTD peak voltage. The obtained value can be cross-checked with the value obtained by the RTD model.

This alone, however, does not give a unique solution for the QW depth and well width, particularly when the uncertain thin AlAs interface roughness is taken into account. High resolution X-ray diffractometry was performed to further narrow down to typically 2 possibilities, solution made possible via layer-parameter linking on similar epitaxial layer on various X-ray modelling software. This concept is summarily shown in Fig. 4. Using this method, we have grown and characterised the 0.6 nm AlAs DBRTS material similar to the optimum described in the previous section, with our preliminary analysis indicating good agreement with TEM.

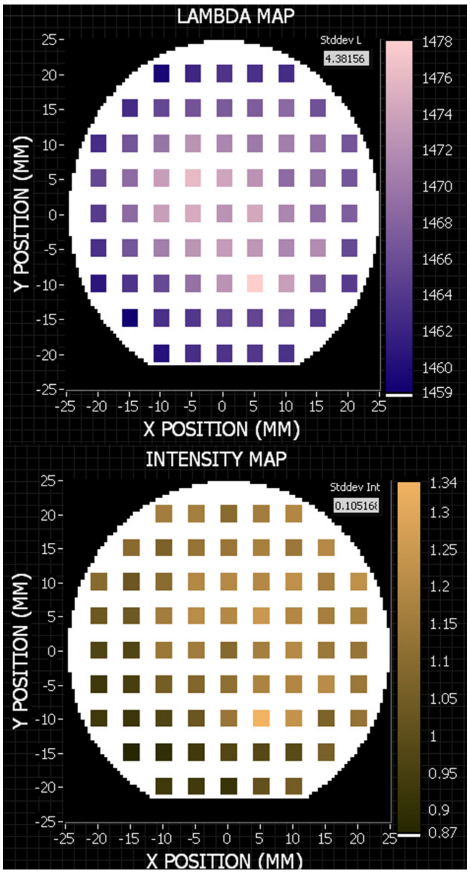

Fig. 3. Low temperature photoluminescence spectra mapping points of a 2-inch diameter InP wafer epitaxially overgrown via MOVPE with an RTD layer structure. Wafer from the National Epitaxy Facility in Sheffield. Wavelength (top), peak InGaAs intensity (bottom)

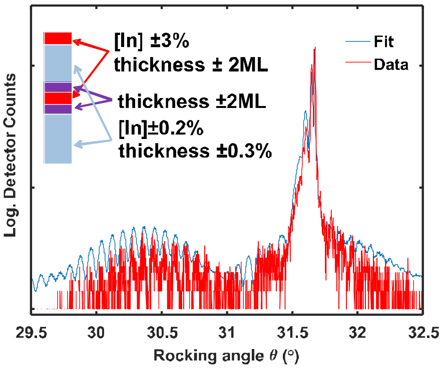

Fig. 4. Sample ω-2θ rocking curve scan (main) and structural parameter sensitivity via parameter-linking (inset). The colour-coding highlights the principle of parameter-linking of similar layers related to intermixing fractions and thickness measures from the growth rate of a calibrated epitaxial process.

V. NEXT STEPS

We have so far reported that we are closing the gap on an epitaxially optimal material for use in THz RTDs. Further confirmation will be performed with the test of fabricated devices. However, high emission powers worthy of including the monolithic RTD emitter/receiver in new systems, are achievable with a new design based on a dielectric resonator antenna[25]. This proposal will be made in the near future, to overcome the limitations of absorption and impedance mismatching, and realise an effective THz emitter. The flow of this process is summarised in Fig. 5

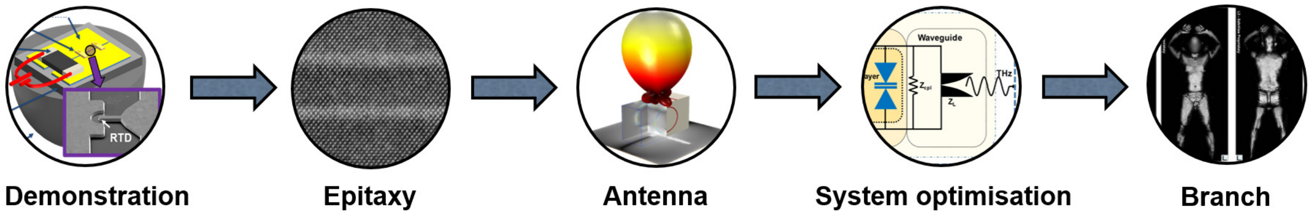

Fig. 5. Roadmap from to the 1st free space THz-emitter RTD technological demonstration in UK (previous work). A novel radiator of THz waves is the centre piece of this project. Further engineering finesse challenges the RTD to feature in field instruments and smartphones of the future. Once this core technology achieves good reproductibility and yield, branching into applications beyond telecommunications can be considered. Schematic from [20], SiO2 antenna image from [26], THz security scanner image from [27].

ACKNOWLEDGEMENTS

In addition to the financial aid, R.B. thanks the RTD community in Glasgow (UoG), and in particular Dr. Edward Wasige. Prof. Asen Asenov and Dr. Vihar Georgiev of the Modelling Group (UoG) for their input on RTD modelling. R.B. also thanks Dr. Neil D. Gerrard (previously Nortel and Thomas Swan & Co Ltd.) for advice regarding MOVPE reactor specifics. We are thankful for all the technical staff at the James Watt Nanofabrication Centre, in particular for the efforts of Mr. David Gourlay.

REFERENCES

[1] S. S. Dhillon et al., “The 2017 terahertz science and technology roadmap,” J. Phys. D. Appl. Phys., vol. 50, no. 4, p. 043001, Feb. 2017.

[2] H.-J. Song, K. Ajito, Y. Muramoto, A. Wakatsuki, T. Nagatsuma, and N. Kukutsu, “Uni-Travelling-Carrier Photodiode Module Generating 300 GHz Power Greater Than 1 mW,” IEEE Microw. Wirel. Components Lett., vol. 22, no. 7, pp. 363–365, Jul. 2012.

[3] A. W. Mohammad et al., “5 Gbps wireless transmission link with an optically pumped uni-traveling carrier photodiode mixer at the receiver,” Opt. Express, vol. 26, no. 3, p. 2884, Feb. 2018.

[4] R. E. Miles, X.-C. Zhang, H. Eisele, and A. Krotkus, Terahertz Frequency Detection and Identification of Materials and Objects, 1st ed. Springer Netherlands, 2007.

[5] T. Shiode, T. Mukai, M. Kawamura, and T. Nagatsuma, “Giga-bit wireless communication at 300 GHz using resonant tunneling diode detector,” in Microwave Conference Proceedings (APMC), 2011 Asia-Pacific, 2011, pp. 1122–1125.

[6] X. Mei et al., “First Demonstration of Amplification at 1 THz Using 25-nm InP High Electron Mobility Transistor Process,” IEEE Electron Device Lett., vol. 36, no. 4, 2015.

[7] T. Otsuji and M. Shur, “Terahertz Plasmonics: Good Results and Great Expectations,” IEEE Microw. Mag., vol. 15, no. 7, pp. 43–50, Nov. 2014.

[8] W. Withayachumnankul and C. Fumeaux, “Photonic crystal traps THz waves,” Nat. Photonics, vol. 8, no. 8, pp. 586–587, Aug. 2014.

[9] T. Mukai, M. Kawamura, T. Takada, and T. Nagatsuma, “1.5-Gbps wireless transmission using resonant tunneling diodes at 300 GHz,” in Tech. Dig. Optical Terahertz Science and Technology 2011 Meeting, 2011, p. MF42.

[10] Lianhe Li et al., “Terahertz quantum cascade lasers with >1 W output powers,” Electron. Lett., vol. 50, no. 4, pp. 309–311, Feb. 2014.

[11] International Telecommunication Union, “Attenuation by atmospheric gases Rec. ITU-R P.676-10,” Geneva, Switzerland, 2013.

[12] E. Wasige et al., “Resonant tunnelling diode terahertz sources for broadband wireless communications,” in Proc. SPIE 10103, Terahertz, RF, Milimeter, and Submilimeter-Wave Technology and Applications X, 2017, p. 101031J.

[13] T. Uno and H. Tabata, “In situ Measurement of Combustion Gas Using Terahertz Time Domain Spectroscopy Setup for Gas Phase Spectroscopy and Measurement of Solid Sample,” Jpn. J. Appl. Phys., vol. 49, no. 4, p. 04DL17, Apr. 2010.

[14] A. Cosentino, “Terahertz and Cultural Heritage Science: Examination of Art and Archaeology,” Technologies, vol. 4, no. 1, p. 6, Feb. 2016.

[15] T. Ouchi et al., “Terahertz imaging system for medical applications and related high efficiency terahertz devices,” J. Infrared, Millimeter, Terahertz Waves, vol. 35, no. 1, 2014.

[16] Y.-D. Hsieh et al., “Dynamic terahertz spectroscopy of gas molecules mixed with unwanted aerosol under atmospheric pressure using fibre-based asynchronous-optical-sampling terahertz time-domain spectroscopy,” Sci. Rep., vol. 6, no. 1, p. 28114, Sep. 2016.

[17] S. Fan et al., “Terahertz non-destructive imaging of cracks and cracking in structures of cement-based materials,” AIP Adv., vol. 7, no. 11, p. 115202, Nov. 2017.

[18] A. Luukanen, R. Appleby, M. Kemp, and N. Salmon, “Millimeter-Wave and Terahertz Imaging in Security Applications,” 2012, pp. 491–520.

[19] K. J. P. Jacobs, B. J. Stevens, O. Wada, T. Mukai, D. Ohnishi, and R. A. Hogg, “A Dual-Pass High Current Density Resonant Tunneling Diode for Terahertz Wave Applications,” IEEE Electron Device Lett., vol. 36, no. 12, pp. 1295–1298, Dec. 2015.

[20] K. J. P. Jacobs, “Development of Resonant Tunnelling Diode Terahertz Emitter,” Ph.D. Dissertation, Dept. of Electronic & Electrical Engineering, The University of Sheffield, 2015.

[21] R. Baba, K. J. P. Jacobs, B. J. Stevens, B. A. Harrison, T. Mukai, and R. A. Hogg, “Fabrication, characterisation, and epitaxial optimisation of MOVPE-grown resonant tunnelling diode THz emitters,” in Proc. SPIE 10111, Quantum Sensing and Nano Electronics and Photonics XIV, 101113A (January 27, 2017), 2017, vol. 10111, p. 101113A.

[22] R. Baba, B. J. Stevens, T. Mukai, and R. A. Hogg, “Epitaxial Designs for Maximizing Efficiency in Resonant Tunneling Diode Based Terahertz Emitters,” IEEE J. Quantum Electron., vol. 54, no. 2, pp. 1–11, Apr. 2018.

[23] K. J. P. Jacobs, B. J. Stevens, T. Mukai, D. Ohnishi, and R. A. Hogg, “Non-destructive mapping of doping and structural composition of MOVPE-grown high current density resonant tunnelling diodes through photoluminescence spectroscopy,” J. Cryst. Growth, vol. 418, pp. 102–110, 2015.

[24] K. J. P. Jacobs et al., “Characterisation of high current density resonant tunneling diodes for THz emission using photoluminescence spectroscopy,” in Proc. SPIE 9758, Quantum Dots and Nanostructures: Growth, Characterization, and Modeling XIII, 97580L (March 15 2016), 2016, p. 97580L.

[25] M. I. Sulaiman and S. K. Khamas, “A Singly Fed Rectangular Dielectric Resonator Antenna With a Wideband Circular Polarization,” IEEE Antennas Wirel. Propag. Lett., vol. 9, pp. 615–618, 2010.

[26] COMSOL AB, “Dielectric Resonator Antenna Application ID: 12042,” 2016. [Online]. Available: https://www.comsol.fi/model/dielectric-resonator-antenna-12042. [Accessed: 12-May-2018].

[27] L-3 Technologies, “SafeViewTM Compact advanced imaging system,” Security & Defense Systems, 2012. [Online]. Available: http://safe-view.com/advancedimaging/safeview.htm. [Accessed: 01-Jun-2018].